

## Research Article



## Fabrication of Nanofibres by Electrospinning using Silk Sericin-graphene Oxide-nano Zinc Oxide

**Vimalan G, Thirumalai Keerthi Vasan, Pandimadevi M\***

Department of Biotechnology, School of Bioengineering, SRM University, Kattankulathur, India.

\*Corresponding author's E-mail: [pandimadevi2008@gmail.com](mailto:pandimadevi2008@gmail.com)

Received: 21-05-2018; Revised: 28-06-2018; Accepted: 12-07-2018.

### ABSTRACT

In this present work, graphene oxide (GO), nano zinc oxide (nZnO) and silk serine (SS) were used for the fabrication of nanofibres by electrospinning technique. Silk serine is a natural polymer and it was prepared from the silk cocoon, which served as an adhesion material. The optimum condition for fabricating SS/GO/nZnO nanofibers by electrospinning was studied. The prepared nanofibres were analysed for their physical and structural characteristics using Scanning Electron Microscope (SEM), Fourier Transform Infra-Red spectroscopy (FTIR), and X-Ray diffraction (XRD) and antibacterial properties. The mechanical properties and water absorption capacity of the electrospun fibres were examined. The presence of nano zinc particles was confirmed from the SEM. The work highlights the great promises of using GO-ZnO-SS biocomposites nanofibres as a highly effective antibacterial property and water absorption capacity, and can be used as a potential wound healing nanomaterials.

**Keywords:** Silk sericin, Graphene oxide, nano Zinc oxide, electrospinning, nano fibres, biocomposites, antimicrobial activity.

### INTRODUCTION

The wound dressing is one of the most promising medical applications of biomedical industry. Nano biomaterials offer interesting physiochemical and biological properties due to their small size, large surface area and ability to interact with cells and tissues. Wound infection is the major challenge in the field of wound care management since such infections can delay the wound healing, and facilitate improper collagen deposition<sup>1</sup>. Microbes like *Staphylococcus aureus* (*S. aureus*) and *Escherichia coli* (*E. coli*) are the major reason for infection which present in high numbers all around us<sup>2</sup>. At times, even a wound dressing can cause infection, because of the wound dressing-exudate interface, and non-sterility of the wound dressing<sup>3</sup>. Therefore it's necessary to create a wound dressing material that possesses all the necessary properties, such as hemostasis, the moist environment at the wound, allow water and air permeation and prevent from external factors like dust and bacteria and also, promote epithelisation by releasing biological agents to the wounds<sup>4</sup>. Electrospinning is known to be a simple and versatile spinning method to generate polymer or composite nanofibers with diameter ranged from 2nm to several micrometers<sup>5</sup>. They can yield a three-dimensional porous network of nanofibers with high aspect ratio and a large specific surface area by stretching and splitting polymer solution under the high voltage electric field<sup>6</sup>. Because of the high surface area to volume or mass ratio of electrospun fibers, the potential applications of these fibrous materials are wound healing, tissue engineering, and drug delivery in the biomedical area<sup>7</sup>. Ultrathin fibers are produced from a rich variety of materials including polymers, composites, ceramic materials and cellulose acetate via electrospinning<sup>8</sup>. Sericin is a natural, hydrophilic, macromolecular silk protein derived from

silkworm *bombyx mori*. It is found to have antioxidant, antimicrobial, UV-resistant properties, promote wound healing and support cell proliferation even in serum free media. The components of silk cocoon is shown in the Fig. 1. The cocoon filament of the *Bombyx mori* silkworm is composed of two silk proteins: silk fibroin (SF) and silk sericin (SS)<sup>9</sup>. SS is a hydrophilic "glue-like" protein that serves as a binding material for the SF monofilaments<sup>10</sup>. SS is obtained as a waste product from silk industry with a worldwide yield up to 50,000 tons<sup>11</sup>. The sericin protein is made of 18 amino acids most of which have strongly polar side groups such as hydroxyl, carboxyl, and amino groups<sup>12</sup> that enable easy cross-linking, copolymerization, and blending with other polymers to form improved biodegradable materials<sup>13</sup>. SS is a family of proteins synthesized in the middle silk gland of silkworms and stored as an aqueous solution<sup>14</sup>. SS content is 20–30 wt% of the cocoon filament<sup>15</sup>. SS plays important roles in the spinning process of the silkworm and the construction of a robust cocoon shell<sup>16</sup>. More recently, SS-based biomaterials have attracted considerable attentions in the field of research in biomaterial science. These can be easily processed into different forms including films<sup>17</sup>, 3D porous scaffolds<sup>18</sup>, hydrogels<sup>19</sup>, as well as fibers via wet spinning<sup>20</sup> or electrospinning<sup>9</sup> and also have diverse functional groups and variable amino acid compositions which confer many useful bioactive properties<sup>21</sup>. It is a degradable biomaterial with different physiological properties, such as antibacterial activity, antioxidant, ultraviolet protection, moisture absorption, and biocompatibility properties<sup>22</sup>. Both naturally derived and synthetic hydrophilic polymeric materials, which have good biocompatibility, have been intensely researched as biomedical materials<sup>23</sup>. Recently, the electrospun sericin nanofibers are of great interest to be developed as biomedical materials<sup>24</sup>. Unfortunately, despite all these



properties and easy availability, SS is not widely used as a biomaterial due to its major inherent drawbacks. The biggest difficulty of them all is the brittleness of the sericin film<sup>24</sup>. Various efforts have been made to overcome this problem, such as refining the sericin, blending the sericin with other polymers<sup>25</sup>, grafting the sericin with synthetic polymers<sup>26</sup> or adding a plasticizer<sup>27</sup>.

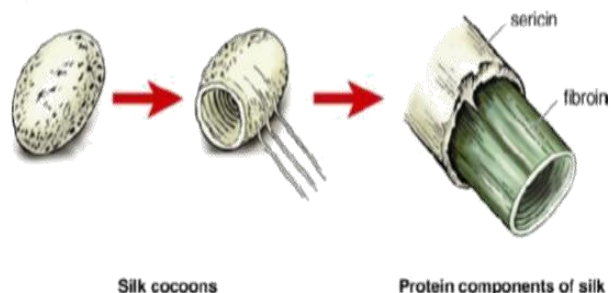


**Figure 1:** Components of silk cocoon

Graphene is a new form of carbon discovered after fullerene and carbon nanotubes<sup>28</sup>. The perfect structure of graphene shows a low level of chemical reactivity, therefore, graphene oxide (GO), one of the derivatives of graphene, which contain a range of reactive oxygen functional groups is considered as a replacement<sup>29</sup>. Graphene oxide (GO), is one derivative of graphene, has been used more frequently in the biological system owing to its relatively higher water solubility and biocompatibility<sup>30</sup>. The completely oxidized compound can then be dispersed in a base solution such as water, and graphene oxide in the form of the solution is then produced<sup>31</sup>. Graphene oxide (GO) based Nanocomposites have raised significant interest in the biomedical area due to their unique structure and excellent mechanical and biomedical properties. GO is produced by the oxidative treatment of graphite by one of the principle methods developed by Brodie, Hummers or Staudenmeir in the year 1958. Graphene oxide's unique structure makes it ideal for drug delivering, anti-microbial and biosensing processes<sup>32</sup>. A stepwise synthesis of graphene oxide nanomaterial from graphite is based on Hummer's method<sup>28</sup>. Various type of polymers have been researched for the preparation of nanocomposite material with GO, including polypropylene<sup>33</sup>, polyvinyl alcohol<sup>34</sup>, poly(3-hydroxybutyrate-co-4-hydroxybutyrate)<sup>35</sup>, alginate<sup>36</sup>, carboxymethyl cellulose<sup>37</sup>, chitosan<sup>38</sup>, starch<sup>39</sup> and others. The expanded graphite is exfoliated into multi-layered or even single-layered sheets<sup>24</sup>. Hummers' Method is a chemical process that can be used to generate graphite oxide through the addition of potassium permanganate to a solution of graphite, sodium nitrate, and sulphuric acid. It is commonly used by engineering and lab technicians as a reliable method of producing quantities of graphite oxide<sup>28</sup>. Various inorganic nanoparticles such as Ag, Au, Fe<sub>3</sub>O<sub>4</sub>, CdS, TiO<sub>2</sub>, SnO<sub>2</sub>, and ZnO are used to hybridize with GO or graphene to obtain antibacterial materials, controlled targeted drug carriers, optoelectronic materials, electrode materials and photocatalytic

materials<sup>11</sup>. Among the graphene-family nanomaterials, GO appears the most suitable for nanocomposite because it has a less tendency to agglomerate itself compared to pristine graphene, and a wide range of functionalities could be introduced<sup>24</sup>. Zinc oxide, which possesses unique physical and chemical properties, such as high chemical stability and high electrochemical coupling coefficient, is known to be a multifunctional material<sup>40</sup>. It is confirmed that the various applications of ZnO nanoparticles depend on upon the control of both physical and chemical properties such as size, size dispersity, shape, surface state, crystal structure, organization onto a support, and dispensability<sup>41</sup>. ZnO nanoparticle is considered as one of the most promising and novel materials because it is believed to be nontoxic and biocompatible and also has various properties like unique catalytic, electrical, electronic, optical and antimicrobial properties and also enhances keratinocyte migration towards the wound site. Also, it is quite cheap and has extensive applications in daily life<sup>42</sup>. ZnO nanoparticle exhibits excellent UV-protection and antibacterial action, which gives rise to its promising application in the water-based coating, ceramic and texture finishing agent, drug carriers and cosmetics and fillings in medical materials<sup>43</sup>. Nano Zinc oxide is well known for its antimicrobial activity and it is used in many cosmetic materials<sup>44</sup>. Previous studies had shown that, on a size scale of <100 nm and at the appropriate concentration, nZnO possesses potential antibacterial activity, but has no adverse effect on normal cells<sup>45</sup>. Nano Zinc Oxide can also enhance keratinocyte migration toward the wound site and promote healing<sup>41</sup>. However, some experts have observed its toxicological effect on target microorganisms<sup>46</sup>. Nanomaterials are made of biopolymers, used for various biomedical, therapeutic and pharmaceutical properties due to its unique small size and a large surface area and ability to interact with tissues and cells<sup>47</sup>. These properties, find several biomedical applications in tissue engineering<sup>48,49</sup>, wound healing<sup>50</sup>, as excipients for drug delivery<sup>51</sup> and also in gene delivery<sup>52</sup>. Various biopolymers have been used as nanocomposites like chitosan<sup>53</sup>, PVP<sup>54</sup>, silk fibroin<sup>55</sup>, silk sericin<sup>56</sup> etc. SS has been used as a nanocomposite material by the addition of various nanoparticles to enhance its properties and to rectify the drawbacks of sericin. In most of the previous studies, SS has been electrospun with various nanoparticles like polyacrylamide<sup>56</sup>, chitin whiskers<sup>57</sup>, cellulose<sup>58</sup>, titanium oxide<sup>2</sup>, calcium ions<sup>59</sup>, graphene oxide<sup>24</sup> and others. One of the important material options for biomaterials such as SS is the formation of Nanofibrous materials<sup>60</sup>. Polymer nanomaterial formed with silk sericin as a base material can have various practical applications in cosmetic industries, biomedical purposes, medical, and textiles and as coating and absorbent membrane<sup>61</sup>. SS is fabricated into nanocomposites along various nanoparticles by electrospinning process<sup>9</sup>. Silk sericin/Graphene oxide Nanocomposites have improved mechanical properties like increased tensile strength, thermal stability along

with enhanced antimicrobial activity<sup>24</sup>. Finding a good solvent for the fabrication of natural polymer is a crucial step for its application. In the case of SF, HFIP or formic acid is used as a solvent<sup>62</sup>. SS however, is highly dissolvable in Trifluoroacetic acid (TFA) which can be further used for electrospinning<sup>9</sup>.

## MATERIALS AND METHODS

### Materials Required

Mulberry silk cocoons were procured from Department of Sericulture, Dharmapuri (TamilNadu, India). Ammonium sulphate, Graphite Flakes (acid treated 99%, Asbury Carbons), Sodium nitrate (98%), Potassium permanganate (99%), Hydrogen peroxide (30% wt), Sulphuric acid (98%), Hydrochloric acid (35%), Sodium hydroxide, Trifluoroacetic acid (TFA) (98%), Zinc acetate dihydrate and Methanol were purchased from SISCOON, India.

### Methodology

#### Preparation of sericin

##### Degumming of raw silk fibers

5 g of silk cocoon was immersed in 100 ml of distilled water in a 250 ml beaker. It was autoclaved for 30 min/ 45 min/ 60 min at 121°C, 13 lb. The degummed water, thus obtained, was filtered and taken for precipitation of sericin.

##### Precipitation of Silk Sericin

Ammonium sulfate (40 g) was added to every 100 mL of the extracted solution to salt out the sericin. The precipitated particles were filtered out and dried in a hot air oven to obtain sericin powder. The obtained sericin powder was preserved for further analysis.

#### Preparation of Graphene Oxide

Graphene oxide was synthesized by Hummers method through oxidation of graphite. Graphite flakes (2 g) and NaNO<sub>3</sub> (2 g) were mixed in 50 mL of H<sub>2</sub>SO<sub>4</sub> (98%) in a 1000 mL volumetric flask kept under at ice bath (0-5°C) with continuous stirring. The mixture was stirred for 2 hrs at this temperature and potassium permanganate (6 g) was added to the suspension very slowly. The rate of addition was carefully controlled to keep the reaction temperature lower than 15°C. The ice bath was then removed and the obtained grey coloured mixture was then stirred at 35°C until it turns into pasty brownish colour and kept under stirring for 2 days. It is then diluted with the slow addition of 100 ml distilled water. The reaction temperature was rapidly increased to 98°C with effervescence. The solution was diluted by adding 200 ml of distilled water with continuous stirring. The solution is finally treated with 10 ml of H<sub>2</sub>O<sub>2</sub> to terminate the reaction which was confirmed by the appearance of yellow color. For purification, the solution was centrifuged with 10% HCl and the sediment was then washed with distilled water repeatedly. The sediment was then vacuum dried to

obtain the graphene oxide powder. Graphene oxide powder was preserved for further analysis.

#### Preparation of Zinc Oxide

Zinc oxide nanoparticles (nZnO) were prepared as follows. 0.1M Sodium hydroxide solution was added dropwise to 0.1M Zinc acetate dihydrate solution with continuous stirring. The solvent used for the preparation was methanol. The precipitated zinc oxide was centrifuged and washed several times with distilled water to remove the impurities and vacuum dried to obtain the Zinc oxide powder.

#### Preparation of SS/TFA/GO/ZnO composite solution

Silk Sericin (SS) powder is dissolved in TFA to form a uniform dilute polymer. To 10ml of TFA solution, 2g of silk sericin is added. 0.5g of GO was first dispersed in 1ml of distilled water and sonicated for 15mins. Different ratios of Sericin and GO such as 2:1, 3:1, 4:1 and 5:1 and 6:1 are prepared with constant ZnO. The GO suspension was added to SS/TFA solution and the final concentration was adjusted to the ratio of 4:1 (Sericin:Graphene oxide). 0.5g nZnO is dissolved in 1ml distilled water before adding them to SS/TFA/GO. The SS/TFA/GO/ZnO was obtained by adding 0.5g ZnO solution to SS/TFA/GO solution. The solution was kept at 25°C in an orbital shaker for 7 days. The ratio of Sericin and graphene oxide was chosen based on the fibre forming capacity on the electrospinning machine.

#### Electrospinning

The electrospinning setup used in this study was from Espin Technologies Pvt. Ltd. It consisted of a syringe and needle, a piece of aluminium collecting drum, a syringe pump, and a high-voltage power supply. The SS/TFA/GO/ZnO solution was placed into a 5ml syringe with a stainless needle (inner diameter 0.3mm), which is connected to the high voltage power supply. The spinning speed of the syringe pump was adjusted within the range 0.003– 0.320cm min<sup>-1</sup>. A high voltage power in the range from 0–20kV was applied to the droplet of SS solution at the tip. A grounded drum with aluminium foil was placed at a distance of 15 cm from the capillary tip. When there was a SS/TFA/GO/ZnO solution droplet at the tip of the needle, a jet was ejected with increasing voltage. The SS/TFA/GO/ZnO nanofibres were formed on an aluminium collecting drum.

#### Characterisation

##### FESEM

The morphology and diameter of SS nanofibers were examined with a scanning electron microscope (Agilent Technologies) at room temperature. Scanning Electron microscopy provides morphology and structure of nanomaterials. The grain size and surface morphology were observed by the field emission scanning electron microscope (FESEM).



## FTIR

It is a technique adopted to obtain an infrared spectrum of absorption, emission, and photoconductivity of a solid, liquid or gas. Also, it can be utilized to quantitative analysis of an unknown mixture. FTIR measurement was employed to investigate the bonding interactions in the composite concoction. It assumes the intensities of the peaks are directly related to the amount of sample present. The change of the structure of the SS nanofibers was measured using Fourier transform infrared spectroscopy (FT-IR, Prestige-21). The spectra of samples were acquired in transmittance mode with a resolution of  $4\text{ cm}^{-1}$ , and spectral range of  $4000\text{--}500\text{ cm}^{-1}$ .

## X-Ray Diffraction

The X-ray diffraction (XRD) is the most widely used technique for general crystalline material characterization. It is used to measure the average spacings between layers or rows of atoms, determine the orientation of a single crystal or grain. The X-ray diffraction pattern of sericin powder was recorded in the  $2\theta$  range of  $10\text{--}35^\circ$  on an X-ray diffractometer (Almelo, The Netherlands). Cu K $\alpha$  radiation was used for the X-ray diffraction study. The crystallinity and crystal phases were determined by X-ray powder diffractometer (XRD) with Cu K $\alpha$  radiation ( $\lambda = 1.54178\text{ \AA}$ ) with Bragg angle ranging from  $208$  to  $658$ .

## Anti-Bacterial activity

The establish anti bacterial properties of SS/GO/nZnO nano fibres, the bacterial cells were cultured aerobically in 25ml of nutrient broth at  $37^\circ\text{C}$  for 24 hours. Sericin, graphene oxide, zinc oxide, negative control and nanofibres were experimented. Disc diffusion method was used for screening the antibacterial activities of the nanofibres. Nutrient agar plates were inoculated with 0.1ml of an appropriate dilution of the tested culture (*Staphylococcus aureus*). SS, GO, ZnO and SS/GO/nZnO nano fibres discs were placed on the surface of the

inoculated plates and incubated at  $37^\circ\text{C}$  for 24hours. The diameter of inhibition zone (mm) including the disc diameter was measured.

## Water absorption capacity

It is of utmost importance, if they are used for biological applications and wound healing. It is used to measure the capacity of film to absorb wound exudates. Prewedged one inch film was placed in 15ml. of distilled water and the weight of the film was noted periodically at first hour, second hour, third hour and 24hour. Every time after noting the weight, the film was placed in fresh water. Water absorption capacity of the film was determined triplicate and calculated using a formula:

$$\% \text{Water absorption capacity} = \left[ \frac{\text{final weight} - \text{initial weight}}{\text{initial weight}} \right] \times 100$$

## RESULTS AND DISCUSSION

### FTIR analysis

The IR spectrum analysis of sericin is as shown in figure 2(a). The peptide group of the proteins gives nine characteristic bands named amides A, B, I, II, III, IV, V, VI, and VII. The amide A band intensity is primarily due to the NH stretching vibration. Amide I is primarily governed by the stretching vibration of the C=O (70–85%) and C-N groups (10–20%) which is found in a frequency range of  $1600\text{--}1700\text{ cm}^{-1}$ . Amide II is found in the  $1510\text{--}1580\text{ cm}^{-1}$  region. Amide II derives mainly from the in-plane N-H bending. The rest of the potential energy arises from the C-N and C-C stretching vibrations. Sericin extracted by the salting-out method showed a peak between  $1600$  and  $1700\text{ cm}^{-1}$  confirmed amide I absorption. Peaks found in the region of  $1510\text{--}1580\text{ cm}^{-1}$  confirmed the presence of the amide II absorption band. The peaks in the region of  $3000\text{--}3500\text{ cm}^{-1}$  are amide A and amide B bands associated with N-H stretching vibrations. The other peaks that are found in the region of  $1500\text{--}400\text{ cm}^{-1}$  may be associated with the complex amide III and V bands<sup>9</sup>.

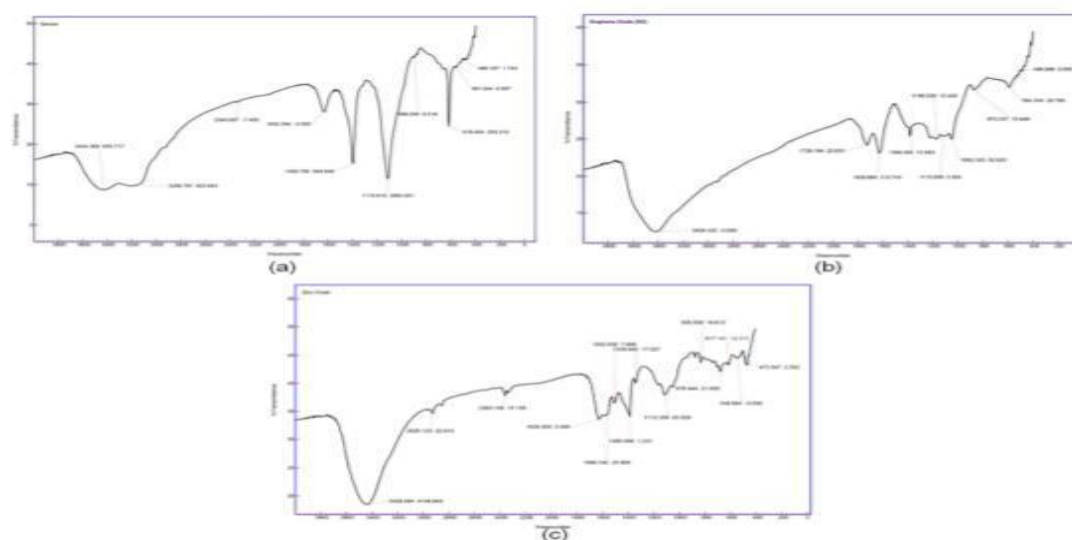


**Figure 2:** FTIR characterisation of (a) SilkSericin (b) Graphene oxide (c) Zinc oxide.

Figure 2 (b) shows that synthesized GO has a peak at  $1081\text{ cm}^{-1}$  which is attributed to the C-O bond, confirming the presence of oxide functional groups after the oxidation process. The peaks in the range of  $1630\text{ cm}^{-1}$  to  $1650\text{ cm}^{-1}$  showed that the C=C bond was remaining after the oxidation process. The absorbed water in GO is shown by a broad peak at  $2885\text{ cm}^{-1}$  to  $3715\text{ cm}^{-1}$ , contributed by the O-H stretch of  $\text{H}_2\text{O}$  molecules. This confirms the fact that the GO is a highly absorptive material<sup>28</sup>.

The composition and quality of the product were analyzed by the FTIR spectroscopy. Figure 2(c) shows the FTIR spectrum which was acquired in the range of  $400\text{--}4000\text{ cm}^{-1}$ . The band at  $523\text{ cm}^{-1}$  is correlated to zinc oxide. The bands at  $3200\text{--}3600\text{ cm}^{-1}$  correspond to O-H mode of vibration and the stretching mode of vibration of CO is observed at  $1431$  and  $1652\text{ cm}^{-1}$ .

#### 4.2 XRD analysis

It has been reported in the literature that sericin is an amorphous macromolecule. The X-ray diffractogram of

the sericin at powder does not show any distinct peak as shown in figure 3(a). This indicates that the extracted sericin powder is amorphous in nature<sup>22</sup>. The diffraction peak at  $2\theta=10^\circ$  is mainly due to the oxidation of graphite. The diffraction peak of pure graphite is generally found around  $26^\circ$ , corresponding to the highly organized layer structure. The XRD pattern for synthesized GO by Modified Hummer's method. The disappearance of the peak at  $26^\circ$  and appearance of the peak at  $10^\circ$  show that the product is completely oxidized after the chemical oxidation and exfoliation, indicating an increase in d-spacing from  $0.34\text{ nm}$  to  $0.82\text{ nm}$ <sup>28</sup>. Figure 3(c) presents the X-ray diffraction pattern of synthesized ZnO powder, which confirms that the synthesized powder is single crystalline and possesses wurtzite hexagonal structures. No other peak related to impurities was detected in the spectrum within the detection limit of the X-ray diffraction, which further confirms that the synthesized powders are pure ZnO<sup>63</sup>.

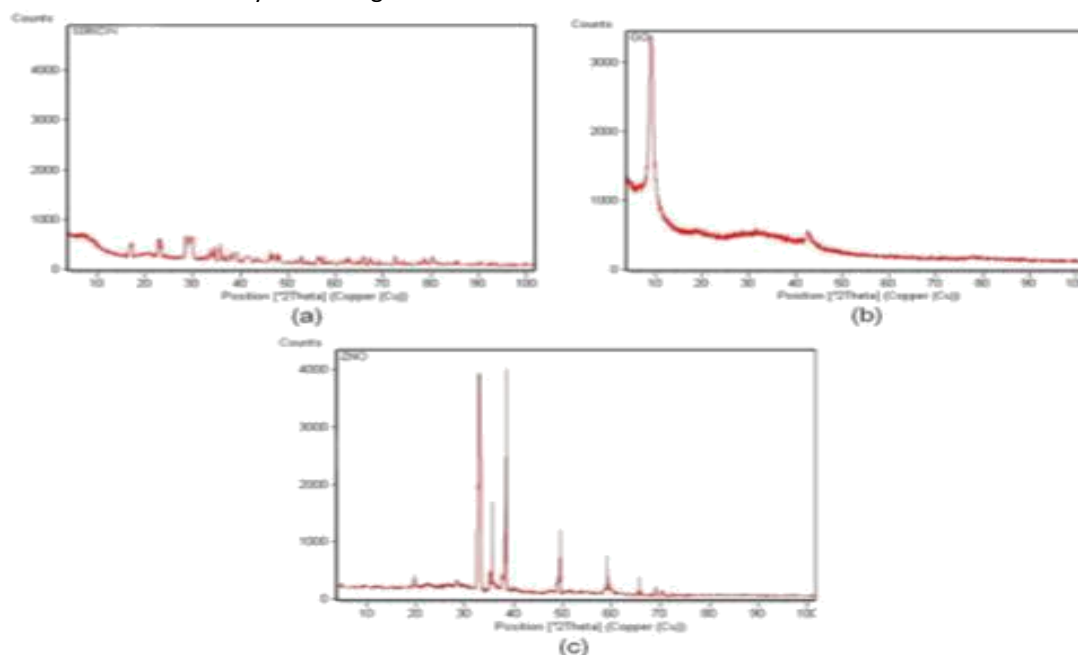


**Figure 3:** XRD analysis of (a) Silk Sericin (b) Graphene oxide (c) Zinc oxide.

#### FESEM analysis

The grain size and surface morphology were observed by the field emission scanning electron microscope (FESEM). Sericin is an amorphous macromolecule. It has no predetermined geometry when viewed under SEM as seen in figure 4(a)<sup>7</sup>. FESEM images of the Graphene Oxide (GO) have well defined and interlinked three-dimensional graphene sheets, forming a porous network that resembles a loose sponge-like structure as shown in figure 4(b)<sup>9</sup>. FESEM images of ZnO nanoparticles are shown in figure 4(c). Bulk particles with high agglomeration are shown. This agglomeration is due to the result of acidic and neutral pH of  $\text{Zn}(\text{OH})_2$  solution during the synthesis process. ZnO nanoparticles are

mostly spherical in shape. The average particle size of ZnO is mostly in the range of  $66.65\text{ nm}$  to  $79.98\text{ nm}$  in diameter<sup>64</sup>.

#### Electrospinning

Electrospinning was conducted under normal atmospheric conditions. This study discloses the fact that the solution properties and processing parameters affect the morphology and diameter of electrospun fibres. In order to obtain proper nanofiber, the following variables including the applied electric field, flow rate of the feedstock solution and drum speed were altered and optimised. The concentration of silk sericin solution for

effective electrospinning was set to be at 20%wt of sericin TFA solution<sup>65</sup>.

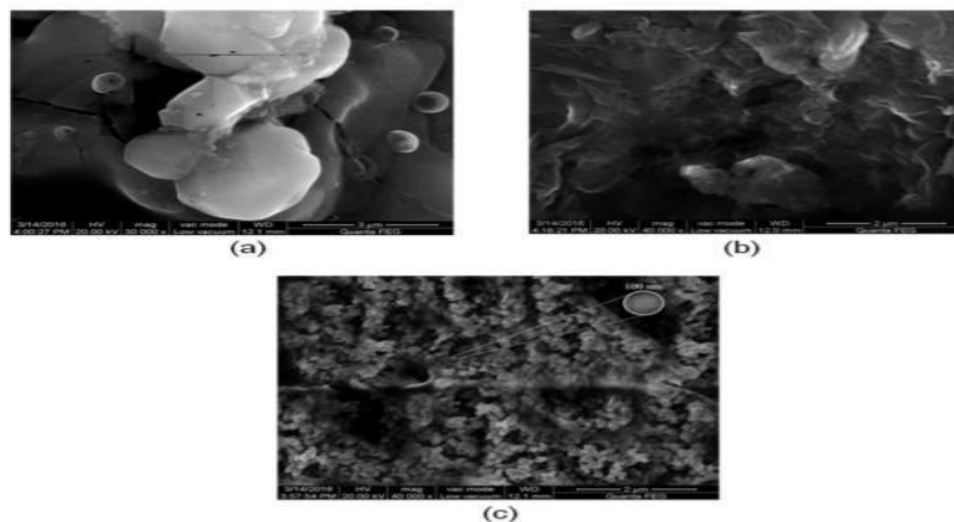


**Figure 4:** FESEM images of (a) Silk Sericin (b) Graphene oxide (c) Zinc oxide.

#### Effect of applied electric field

SS/GO/ZnO nanofibres are produced by electrospinning with TFA at a concentration of 20wt% at different voltages ranging from 10-17kV. SS nanofibers spun at voltages >15kV produced smooth and continuous nanofibers as in figure 6(b) and 6(c). It was observed that the average diameter of nanofibre decreases with increasing voltage. The mean diameter of electrospun nanofiber at 17kV was found in the range of 300-600nm thickness<sup>65</sup>.

#### Effect of flow rate of spinning solution

The ejecting speed of the SS/GO/nZnO solution from the tip of the syringe is controlled by the syringe pump. The flow rate of the sample was adjusted from 2.1 to 2.8 ml hr<sup>-1</sup>. Figure 5(b) and 5(c) show SEM images of SS/GO/ZnO nanofibres spun at 17kV at different flow rates. Continuous and fine SS/GO/ZnO nanofibers can be produced at higher flow rate conditions of above 2.5 ml hr<sup>-1</sup>. The optimum flow rate to produce fine and smooth uniform nanofiber<sup>65</sup> was obtained around 2.8 ml hr<sup>-1</sup>.

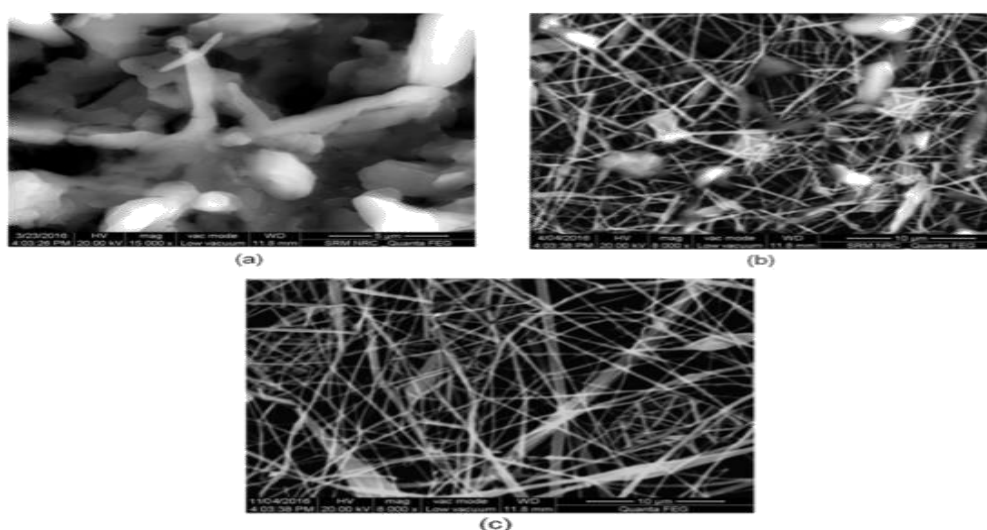


**Figure 5:** FESEM image of SS-GO-ZnO at constant spinning distance different voltage and flow rate (a) 10 kV; 2.1 ml /hr (b) 17 kV; 2.5 ml/hr (c) 17 kV; 2.8 ml/hr

#### Morphology of SS/GO/ZnO nanocomposites

##### FTIR analysis

The SS nanofiber spun from SS solution showed absorption peak at 1728 cm<sup>-1</sup> (amide I), and 1566 cm<sup>-1</sup> (amide II), assigned to the random coil conformation (figure 6). In addition, a sharp absorption band exhibited

for SS nanofiber at around 1200 cm<sup>-1</sup> was due to the TFA. These FTIR results suggest that the  $\beta$ -sheet structure of sericin powder breaks in the dissolution process with TFA<sup>9</sup>. The FTIR spectrum also reveals the formation of GO in the SS/GO/nZnOfibers<sup>9</sup>, as functional groups such as -OH (3434 cm<sup>-1</sup>), epoxy -C-O (1384 cm<sup>-1</sup>) and alkoxy -C-O (1080 cm<sup>-1</sup>) can be found in figure 6. These results

indicate that the exfoliated GO prepared by the modified Hummer’s method was successfully fabricated into the nanofibers along with SS and ZnO. The FTIR spectrum of nanofiber also showed the presence of ZnO at a peak at  $496\text{ cm}^{-1}$  which are due to the stretching vibration of the Zn-O bond in ZnO particles. Furthermore, the vibration of the Zn-O bond is interfered with by the SS peptide coating of ZnO particles<sup>63</sup>, leading to the distinct peak of  $548\text{ cm}^{-1}$ .

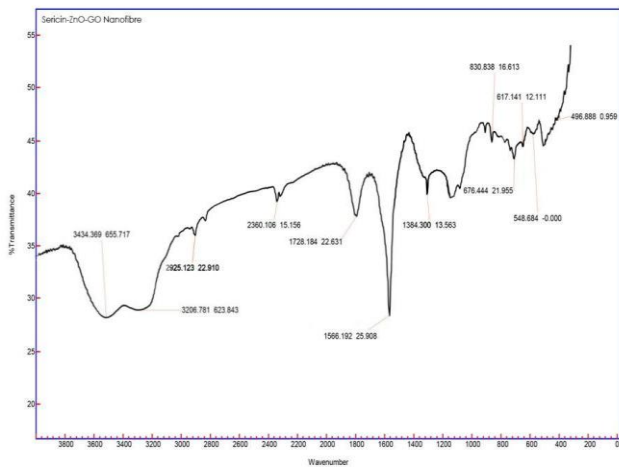


Figure 6: FTIR analysis of SS-GO-ZnO Nanofiber

**XRD analysis**

XRD patterns of SS/GO/nZnO nanofibers were shown in Figure 7. No apparent characteristic peaks were observed in the pattern of composite nanofibers. The crystallization found in GO and nZnO as of Figure 7 was hindered during the electrospinning process and both of the polymers were in the amorphous forms in the composite nanofibers<sup>66</sup>.

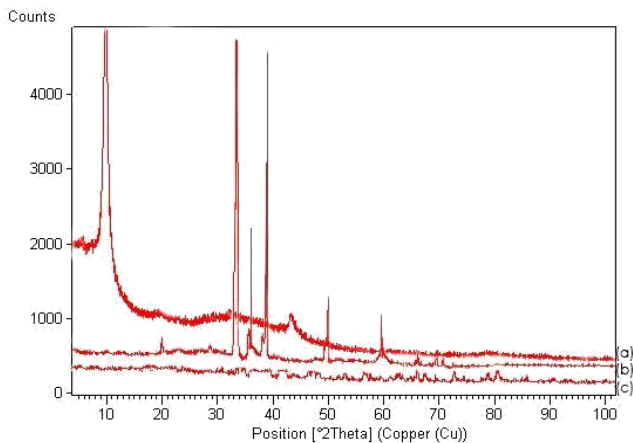


Figure 7: XRD characteristics of (a) Graphene oxide (b) Nano Zinc Oxide (c) SS-GO-ZnO Nanofiber.

**Antibacterial assay**

Growth inhibitory property of SS/GO/nZnO was tested on a bacterial species (*Staphylococcus aureus*). The results in figure 8 and table 1 showed that Silk Sericin, Graphene oxide, nanoZinc oxide and SS/GO/nZnO nanofibers possess antibacterial activity, which was confirmed by the appearance of a clear zone around the loaded sample.

The table below represents the zone of inhibition for corresponding microbe<sup>67</sup>.

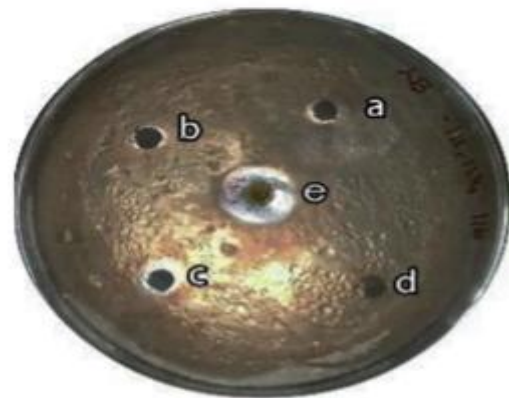


Figure 8: Anti-microbial activity of *Staphylococcus aureus*

Table 1: Table representing antimicrobial activity (zone of inhibition)

	Samples	Zone of inhibition (dia in cm)
a)	Sericin	0.6
b)	Graphene oxide	0.7
c)	Zinc oxide	1.2
d)	Negative control	0
e)	Nanofiber	1.7

**Water Absorption Capacity**

The water absorption capacity of composite films was significantly increased with increase in sericin concentration, which may be due to hydrophilicity and swelling properties of sericin<sup>68</sup>. A composite fibres of 4:1 ratio of SS/GO with constant of 0.5ml of ZnO has shown maximum water absorption capacity among all the prepared film (Fig.9). The biocomposites showed nearly 100% water absorption after 24 hours and depending upon the ratio of sericin and grapheme oxide, the rate of absorption varies.

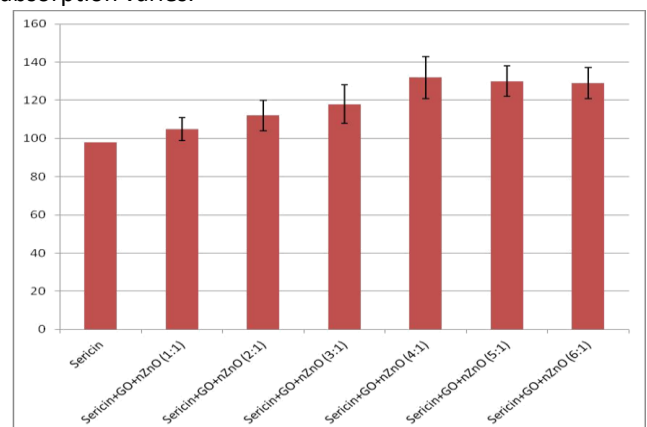


Figure 9: % Water absorption of Sericin biocomposites after 24 hrs. All results were given in mean $\pm$ SD.

## CONCLUSION

Extraction of Silk Sericin from Silk cocoon and synthesis of Graphene oxide from Graphite and Nano Zinc oxide from Zinc acetate dihydrate were performed. Their structural and physical properties were studied by FTIR, XRD, FESEM. Then Sericin/Graphene oxide/Nano Zinc oxide Nanocomposites were fabricated by electrospinning process to form nanofibers. The optimum conditions for fabricating SS/GO/nZnO nanofibers were found to be at 20 wt% Sericin TFA solution, the voltage of 17,000V, Syringe distance of 12cm, drum speed of 600rpm and a flow rate of 2.8ml/hr. The presence of SS, GO, and nZnO in the electrospun nanofibers was confirmed using FTIR and XRD. The mean diameter of the electrospun nanofibers was found in the range of 300nm-600nm from the FESEM analysis. In this study, the prepared SS/GO/nZnO nanofibers showed increase in the physical properties for silk sericin based composite material. The fabricated SS/GO/nZnO nanocomposite could be used as a biopolymer nanomaterial in wound dressing, scaffolds and in the biomedical applications.

## REFERENCES

- Gurtner C, Werner S, Barrandon Y, Longaker MT, Wound repair and regeneration, *Nature*, 453, 2008, 314-21.
- Doakhan S, Montazer M, Rashidi A, Moniri R, Moghadam MB, Influence of sericin/TiO<sub>2</sub> nanocomposite on cotton fabric: PART 1. Enhanced antibacterial effect, *Carbohydrate Polymers*. 94, 2013, 737–748.
- Liza, Ovington G, Advances in wound dressings, *Clinics in Dermatology*, 25, 2007, 33–38.
- Joshua S. Boateng, Kerr H. Matthews, Howard N.E. Stevens, Gillian M. Eccleston, Wound Healing Dressings and Drug Delivery Systems: A Review, *Journal of Pharmaceutical Sciences*, 97 (8), 2008, 2892-2923.
- Zhang W, Chen M, Diao. G, Electrospinning  $\beta$ -cyclodextrin/poly (vinyl alcohol) nanofibrous membrane for molecular capture, *Carbohydrate Polymers*, 86(3), 2011, 1410–1416.
- Ojha SS, Fabrication and characterization of electro spun chitosan nanofibers formed via templating with polyethylene oxide, *Bio macromolecules*. 9(9), 2008, 2523-2529.
- Welle A, Koger M., Doring M., Niederer K., Pindel E, Chronakis I.S, Electrospun aliphatic poly (carbonate)s nanofibers as tailored tissue scaffold materials, *Biomaterial*, 28, 2007, 2211-2219.
- Keiichi Yoshimatsu, Lei Ye, Johanna Lindberg, Ioannis, Chronakis S, Selective molecular absorption using electrospun nanofiber affinity membranes, *Biosensors and Bioelectronics*, 23, 2008, 1208-1215.
- Majibur Rahman Khan MD, Masuhiro Tsukada, Xianhua Zhang, Hideaki Morikawa, Preparation and characterization of electro spun nanofibers based on silk sericin powders, *J. Mater Sci*. 48, 2013, 3731-3736.
- Yu-Qing, Yan M, Yun-Yue X, Wei-De S, Jian-Ping M, Silk sericin-insulin bioconjugates : Synthesis, characterization and biological activity, *J Controlled Release*, 115, 2006, 307-315.
- Srinivas Namratha, D Roopini Kumar, Merchan Nandan, Subramanya Disha, Pruthvika, Jain Puja, Mariappan L, Rao R Ramachandra, Rajyalakshmi M, Extraction & characterization of sericin and its immobilization of hydroxylapatite nanoparticles for tissue engineering applications, *International journal of ChemTech Research*, 4, 2014, 2117-2124.
- Periyasamy S Gulrajani M.L, Gupta D, Preparation of multifunctional mulberry silk fibroin having hydrophobic and hydrophilic surface using VUV excimer lamp, *Surface coating technology*, 201, 2008, 7286-7291.
- Zhang Yu-Qing, Application of natural silk protein in biomaterials, *Biotechnology Advances*. 20(2), 2002, 91-100.
- Suwantong O, Electrospun cellulose acetate fiber mats containing curcumin and release characteristic of the herbal substance, *Polymer*, 48, 2007, 7546-57.
- Zhang, Y.-Q., Yu, X.-H., Shen, W.-D., Ma, Y.-L., Zhou, L.-X., Xu, Mechanism of fluorescent cocoon sex identification for silkworms *Bombyx mori*, *Science China Life Sciences*, 53, 2010, 1330–1339.
- Rui Zhao, Xiang Li,, Bolun Sun, Ying Zhang, Dawei Zhang, Zhaohui Tang, Xuesi Chen, Ce Wang, Electrospun chitosan/sericin composite nanofibers with antibacterial activity as potential wound dressings, *International Journal of Biological Macromolecules*, 68, 2014, 92-97.
- Jin, H. J, Park, J, Karagiorgiou, V, Kim, U. J, Valluzi, R, Cebe, P, Kaplan, DL, Water-Stable Silk Films with Reduced  $\beta$ -Sheet Content, *Advanced Functional Materials*. 15(8). 2005, 1241-1247.
- Kim H. W., Knowles J. C., Kim HE, Development of hydroxyapatite bone scaffold for controlled drug release via poly( $\epsilon$ -caprolactone) and hydroxyapatite hybrid coatings, *J. Biomed. Mater. Res. Part B: Appl. Biomaterial*, 70, 2004, 240–249.
- Kim S, Kim H, Park S, Ki. I. , Lee S, Lee T, Kim S, Behavior in electric fields of smart hydrogels with potential application as bio-inspired actuators, *Smart Materials & Structures*, 11, 2005, 1-5
- Yan J.P., Zhou G.Q, Knight D.P. Shao Z.Z, Chen X, Wet-spinning of regenerated silk fiber from aqueous silk fibroin solution: Discussion of spinning parameters, *Bio macromolecules*, 11, 2010, 1–5.
- Lamboni L, Gauthier M, Yang G, Wang Q, Silk sericin: A versatile material for tissue engineering and drug delivery, *Biotechnol Adamces*, 33(8), 2015, 1855-67.
- Gulrajani ML, Brahma KP, Kumar Senthil P, Roli Purwar, Application of silk sericin to polyester fabric, *Journal of Applied Polymer Science*, 10, 2008, 2796-2805.
- Drury JL, Mooney DJ, Hydrogels for tissue engineering: Scaffold design variables and applications, *Biomaterials*, 24, 2003, 4337-4351.
- Haesung Yun, Moo Kon Kim, Hyo Won Kwak, Jeong Yun Lee, Min Hwa Kim, Eui Hwa Kim, Ki Hoon Lee, Preparation and characterization of silk sericin/glycerol /graphene oxide nanocomposite film, *Journal of Fibers and Polymers*, 4, 2013, 2111-2116.
- Wang L, Shansky J, Borselli C, Mooney D, Vandenburg H, Design and fabrication of a biodegradable, covalently crosslinked shape-memory alginate scaffold for cell and growth factor delivery, *Tissue Eng Part A*, 18, 2012, 2000-2007.
- Hu K, Cui FZ, Lv Q, Ma J, Feng QL, Xu L, Preparation of fibroin/recombinant human-like collagen scaffold to promote fibroblasts compatibility, *J Biomed Mater Res Part A*, 84, 2008, 483-90.
- Zhang H, ddeng I, Yang M, Min s, Yang L, Zhu L, Enhancing Effect glycerol on the tensile properties of Bombyx mori cocoon sericin films, *J of Molecular sciences*, 1, 2011, 3170-3181.
- Paulchamy B. Arthi G, Lingesh BD, A simple approach to stepwise synthesis of graphene oxide nanomaterial, *Journal of Nanomedicine & Nanotechnology*, 16, 2015, 2-4.
- Yang X, Multi functional graphene oxide based anti cancer drug-carrier with dual targeting function and pH-sensitivity, *J. of Material chemistry*, 21, 2011, 448-3454.
- Feng L, Liu Z, Graphene in biomedicine: opportunities and challenges, *Nanomedicine (Lond)*, 6, 2011, 317-324.
- Rodriguez-Lozano FJ, Garcí a-Bernal, Aznar-Cervantes, RosRoca MA, Effects of composite films of silk fibroin and graphene oxide on the proliferation, cell viability and mesenchymal phenotype of periodontal ligament stem cells, *J Mater Sci: Mater Med*, 25, 2014, 2731–2741.
- Shen H., Zhang L, Liu M, Zhang, Biomedical applications of Graphene, *Theranostics*, 2(3), 2012, 283–294.



33. Sánchez-Valdes, A.G. Zapata-Domínguez, J.G. Martínez-Colunga, J. Méndez-Nonell, Influence of functionalized polypropylene on polypropylene/graphene oxide nanocomposite properties, *Polymer Composites*, 2016. DOI: 10.1002/pc.24077.
34. Liang N., Sun S, Li X, Piao H, Cui F,  $\alpha$ -Tocopherol succinate-modified chitosan as a micellar delivery system for paclitaxel: Preparation, characterization and *in vitro/in vivo* evaluations, *International Journal of Pharmaceutics*, 423 (2), 2012, 480–488.
35. Sridhar, Lee I, Chun HH, Park H, Graphene reinforced biodegradable poly(3-hydroxybutyrate-co-4-hydroxybutyrate) nano-composites. *V EXPRESS Polymer Letters*, 7(4), 2013, 320-328.
36. Yongqiang He, Nana Zhang, Qiaojuan Gong, Haixia Qiub, Wei Wang, Yu Liu, Jianping Gao, Alginate/graphene oxide fibers with enhanced mechanical strength prepared by wet spinning, *Carbohydrate Polymers*, 8, 2012, 1100-1108.
37. Mithilesh Yadav, Rhee KY, Jung HI, Park SJ, Eco-friendly synthesis, characterization and properties of a sodium carboxymethyl cellulose/graphene oxide nanocomposite film. *Cellulose*, 20(2), 2013, 687-698.
38. Bao H, Pan Y, Ping Y, Sahoo NG, Wu T, Li L, Li J, Gan LH, Chitosan-functionalized graphene oxide as a nanocarrier for drug and gene delivery, *7(11)*, 2011, 1569-78.
39. ang Q., Saito T., Isogai A. (2012) Facile fabrication of transparent cellulose films with high water repellency and gas barrier properties. *Cellulose*. 19, 1913–1921.
40. Liu XG, Geng DY, Meng H, Shang PJ, Zhang ZD, Microwave-absorption properties of ZnO-coated iron nano capsules, *Appl.Phys.Letter*, 92, 3008, 173117.
41. Sudheesh Kumar PT, Lakshmanan Vinoth Kumar, TV Anilkumar, C Ramya, P Reshmi, AG Unnikrishnan, Shantikumar Nair V, Jayakumar R, Flexible and microporous chitosan hydrogel/nano Zn composite bandages for wound dressing: *in vitro* and *in vivo* evaluation, *ACS applied material and interfaces*, 4, 2012, 618–2629.
42. Sudeep, Narayanan TN, Aswathi G, Shaijumon, Ajayan, Covalently interconnected 3-D Graphene-oxide solids, *ACS Nano*, 7, 2013, 7034-7040.
43. Tang Z., Geng D., Lu G, Size-controlled synthesis of colloidal platinum nanoparticles and their activity for the electrocatalytic oxidation of carbon monoxide. *J. Colloid Interf. Sci.* 287(1), 2005. 159-66.
44. Xie Y, He Y, Irwin PL, Jin T, Shi X, Antibacterial activity and mechanism of action of zinc oxide nanoparticles against *Campylobacter jejuni*. *Appl. Environmental Microbiology*, 77, 2011, 2325-2331.
45. Nair R, Kumar D.S. Chapter 10: Plant diseases-control and remedy through nanotechnology. Tuteja N, Gill SS (eds) *Crop improvement under adverse conditions*, 2013;231-243.
46. Mosaad A. Abdel-Wahhab, Hanaa H. Ahmed and Mohamad M. Hagazi, Prevention of aflatoxin B1-initiated hepatotoxicity in rat by marine algae extracts, *Journal of Applied Toxicology*, 26, 20006, 229-238.
47. Partha R., Mitchell L.R., Lyon JL, Joshi PP, Buckysomes, Fullerene-based nanocarriers for hydrophobic molecule delivery, *ACS Nano* 2. Conyers J.L. 20008, 1950- 1958.
48. Jayakumar R, M Prabakaran , RL Reis , JF Mano, Graft copolymerized chitosan-Present status and applications, *Carbohydrate Polymer*, 62, 2005, 142-158.
49. Madhumathi K, Binulal N. S., Nagahama H, Tamura H, Shalumon K. T, Selvamurugan N., Nair SV, Jayakumar R, Preparation and characterization of novel  $\beta$ -chitin–hydroxyapatite composite membranes for tissue engineering applications, *International Journal of Biological Macromolecules*, 4, 2009, 1-5.
50. Madhumathi K, Sudheesh Kumar PT, Abilash S, Sreeja V, Tamura H, Manzoor K, Nair SV, Jayakumar R, Development of novel chitin/nanosilver composite scaffolds for wound dressing applications, *J Mater Sci Mater Med*, 21, 2010, 807-813.
51. Jayakumar R, New N, Tokura S, Tamura H, Sulfated chitin and chitosan as novel biomaterials, *International Journal of Biological Macromolecules*, 40, 2007, 175–181.
52. Jayakumar R., Chennazhi K. P., Muzzarelli R. A. A, Tamura H., Nair S. V, Selvamurugan N, Chitosan conjugated DNA nanoparticles in gene therapy, *Carbohydrate Polymers*, 79(1), 2010, 1–8.
53. Narges Naseri, Aji P. Mathew, Lenart Girandon, Mirjam Frohlich, Kristina Oksman, Porous electrospun nanocomposite mats based on chitosan–cellulose nanocrystals for wound dressing: effect of surface characteristics of nanocrystals. *Cellulose*, 22, 2015, 521–534.
54. Kokabi. M, PVA-clay nano-composite hydrogels for wound dressing, *Eur. Polym. J.*, 43, 2007, 773-781.
55. Feng X. X., Zhang L. L, Chen J. Y., and Zhang JC, New insights into solar UVprotectives of natural dye, *Journal of Cleaner Production*, 15(4), 2007, 366-372.
56. Kundu, B, Kundu, SC, Silk sericin/ polyacrylamide *in situ* forming hydrogels for dermal reconstruction, *Biomaterials*, 33(30), 2012, 7456-7467.
57. Wongpanit P, Preparation and characterization of chitin whisker-reinforced silk fibroin nanocomposite sponges, *Eur. Polym. J.*, 43, 2007, 4123-4135.
58. Kongdee A, Bechtold T, Teufel L, Modification of cellulose fiber with silk sericin *J.Appl.Poly.Sci.*, 96, 2005, 1421-1428.
59. Yang YY, Hu H., Wang X., Yang F., Shen H., Xu FJ., Acid-labile poly(glycidyl methacrylate)-based star gene vectors. *ACS Appl Mater Interfaces* 7, 2015, 12238–12248.
60. Yamamoto H., Demura T., Morita M., Banker G. A., Tani T., Nakamura S, Differential neurite outgrowth is required for axon specification by cultured hippocampal neurons. *J. Neurochem*. 123, 2012, 904–910.
61. Rangi A, Jajpura A, The Biopolymer Sericin: Extraction and Applications, *J Textile Sci Eng.*, 5, 2015, 188-195.
62. Zhao-Xiang Zhang, Xiao-Wei Zhang, and Shu-Sheng Zhang, Heart-cut capillary electrophoresis for drug analysis in mouse blood with electrochemical detection, *Analytical Chemistry*, 387(2), 2009, 171-177.
63. Rizwan Wahab, S.G. Ansari, Y.S. Kim, H.K. Seo, G.S. Kim, Gilson Khang, Hyung-Shik Shin, Low temperature solution synthesis and characterization of ZnO nano-flowers. *Materials Research Bulletin*, 42, 3007, 1640–1648.
64. Huang Z, Zheng X, Yan D, Yin G, Liao X, Kang Y, Yao Y, Huang D, Hao B, Toxicological effect of ZnO nanoparticles based on bacteria., *Langmuir*, 24(8), 2008, 4140-4.
65. Yongpei Hu, Qin Zhang, Renchuan You, Lingshuang Wang, and Mingzhong Li, The Relationship between Secondary Structure and Biodegradation Behavior of Silk Fibroin Scaffold, *Advances in Materials Science and Engineering*, 2012, DOI.org/10.1155/2012/185905.
66. Qingbiao Yang, Zhenyu Li, Youliang Hong, Yiyang Zhao, Shilun Qiu, CE Wang, Yen Wei, Influence of Solvents on the Formation of Ultrathin Uniform Poly(vinyl pyrrolidone) Nanofibers with Electrospinning, *Journal of Polymer Science, Part B*. 42, 2004. 3721-3726.
67. Linlin Zhong, Kyusik Yun, Graphene oxide modified ZnO particles : Synthesis, characterization and antibacterial properties, *J of Nanomedicine*, 4, 2015, 79–92.
68. Cao Y, Wang B, Biodegradation of Silk Biomaterials, *Int J Molecular Science*, 10, 2009, 1514-1521.

Source of Support: Nil, Conflict of Interest: None.

